IASJ
المجلات الاكاديمية العراقية

Tikrit Journal of Pure Science
ISSN: 1813 – 1662 (Print) --- E-ISSN: 2415 – 1726 (Online)

Journal Homepage: http://tjps.tu.edu.iq/index.php/j

Nickel and titanium metals for the hydrogen evolution reaction in water electrolysis: A comparative study

Aya Awas Saad, Farkad Ali Lattieff
Department of energy engineering, college of energy, University of Baghdad, Baghdad, Iraq

https://doi.org/10.25130/tjps.v28i1.1267

ARTICLE INFO.

Article history:
-Received: 3 / 10 / 2022
-Accepted: 30 / 10 / 2022
-Available online: 20 / 2 / 2023

Keywords: Alkaline electrolysis, Titanium metal, Nickel metal, Hydrogen production, High voltage, power ohmic loss, SEM, EDX.

Corresponding Author:
Name: **Aya Awas Saad**
E-mail:
Tel:

ABSTRACT

This work investigated experimentally and theoretically the I-V output change, the hydrogen production, and the efficiency of Ti and Ni metals as substrates for water electrolysis systems. To make optimization between the candidate electrodes, seven configurations of Ni-Ti, Ti-Ti, and Ti-Ni with three KOH solutions of 10, 20, and 30 % wt (weight KOH gm/weight water gm) as an electrolyte were conducted as a cathode-anode system. The selected electrodes were examined by scanning electron microscopy (SEM) and energy dispersive (EDX) to study their surface morphology and element composition. According to experimental findings, when the cell voltage of 5 V is applied, the hydrogen production from the Ti-Ti (20%KOH) and Ni-Ti (20% and 30% KOH) electrodes reach an optimal value of 6331 cm^3, which is significantly higher than the hydrogen production from the other electrodes at the same voltage. The Ni-Ti electrode with a 10% KOH content had the maximum efficiency (72%), and the Ni-Ti electrode with a 30% KOH content had the lowest efficiency (61%), both at 3V for the cell. This study demonstrates that the Ni-Ti system can be the most suitable source for hydrogen evolution rather than the other arrangements when the appropriate mixing ratio of 20 % KOH solution is prepared before the electrolysis process.

1- Introduction

Renewable energy applications have become an integral part of present-day living. With the changing lifestyle, the demand and supply of renewable energy systems have gradually increased. As one of the renewable energy sources, a water electrolysis unit powered by photovoltaic cell electricity is the most common means for hydrogen generation purposes [1-3]. Hence, alkaline water electrolysis can be a good alternative to conventional steam reforming [4-9]. However, it is not commercially competitive with the steam reforming method [10]. Further development research is still required for improvement in the existing design to increase the catalytic activity of the cathode and the anode, consequently increasing the overall performance of the system and reducing the system unit cost [11-15]. Despite their high resistivity toward oxidation, expensive noble's materials such as platinum give limitations in the water-splitting technology due to their high price and environmental issues such as corrosion [16-18]. To reduce the overall cost, diaphragm issues, and its complex assembly, an alternative of growing interest is diaphragm-free AEC. These types of electrolyzers use water-electrolytes of potassium hydroxide (KOH) or sodium hydroxide (NaOH) in a range of 20-30 % wt [19]. The need for integration between Ni and Ti metal electrodes as a cathode-anode system seems consistent with the alkaline electrolyte of the KOH solution. Hydrogen generation using Ti and Ni metal electrodes via water electrolysis has been the subject of interest to several research works [20-25]. The overpotential of Ni element for hydrogen and oxygen reaction was reported by Alejandro et al. [26]. This study was carried out using a direct-current powered electrolysis system of high KOH concentration solution. Raney Ni and stainless steel 316L were used as the cathode and anode, which were inserted to run for one month in a locally monopolar cell at 300 mA/cm^2. A significant decrease in overpotential of 550 mV at 1000 mA/cm^2 was estimated. They suggested that Ni is not suitable to be used as an anode catalyst due to its strong fluctuation with time. Cinthia et al. [27] prepared Ti-TiO$_2$ catalysts in alkaline electrolytes as support for oxidation-reduction reactions. A good electrocatalyst activity with low stability was confirmed toward the oxygen reduction reaction. However, the research on optimization toward hydrogen production, particularly those of precursor non-Nobel materials, as well as those that have been worked for a long time without disturbance, are limited in the literature. To the best of the authors' knowledge, there is no comprehensive study that has been conducted to address the comparison of such matters, Ti and Ni. The production process involves the interference of different parameters that need to be revealed to overcome limitations and allow process optimization. Therefore, the kinetics parameters such as I-V response, cumulative hydrogen generation, water electrolysis potential, power ohmic loss, and cumulative time for current loss are all determined, discussed, and revealed in this investigation. Dependent algebraic equations were adopted to calculate the cumulative hydrogen generation from the I-V data.

2- Alkaline electrolysis system (AEC)

In alkaline water electrolysis, water is electrochemically split into hydrogen and oxygen at the cathode and anode, respectively [28]. As illustrated in Fig 1. the cathode and the anode are immersed in a KOH electrolytic solution. The cell is connected to a DC power supply or any renewable energy source that transfers the current to the cathode (negative electrode). Water molecules are reduced to produce hydrogen atoms and hydroxide ions.

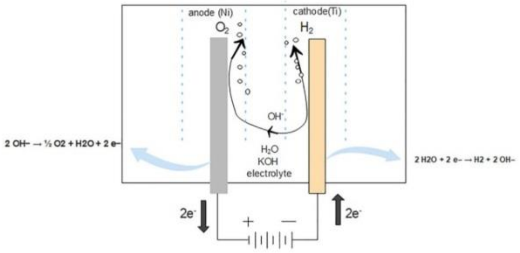

Fig. 1: Conventional alkaline water electrolyzer diagram

The hydroxide ions then make their route to the anode (positive electrode) where they are oxidized to produce oxygen gas and a water molecule. Generally, the water electrolysis reaction for alkaline electrolyte is divided into two half-reactions, the cathode half-reaction, and the anode half-reaction, and are explained by [29] as follows:

Cathode: $2\ H_2O + 2\ e^- \rightarrow H_2 + 2\ OH^-$ ($E^0 = -0.83$ V vs. SHE) …. (1)

Anode: $2\ OH^- \rightarrow \frac{1}{2}\ O_2 + H_2O + 2\ e^-$ ($E^0 = 0.40$ V vs. SHE) …. (2)

Overall reaction: $H_2O_{(l)} \rightarrow \frac{1}{2}\ O_{2(g)} + 2\ H_2$ ($E^0 = -1.23$ V vs. SHE) ….(3)

A basic measurement tool that characterizes AEC is the polarization curve, which consists of three parts as shown in Fig.2. Activation polarization is a rate-determining step that is related to the rate of electrochemical reaction occurring at the surface of the electrode. This is considered a barrier that is overcome when enough voltage (greater than the theoretical voltage) is applied. Ohmic polarization is directly related to the AEC resistances that include an electrode, electrolyte, and gas separator resistances. Concentration polarization happens at high current densities where the transfer of reactants to and from the electrode is very slow leading to a mass transfer-limiting step.

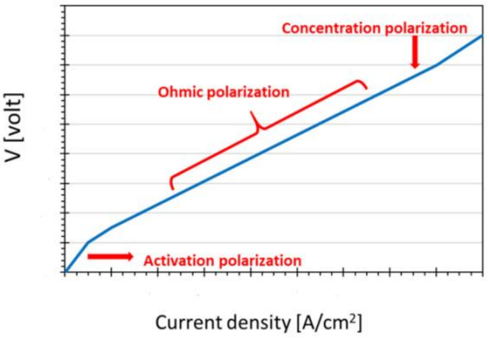

Fig. 2: Typical AEC polarization curve [30]

To study the efficiency of the electrolyzer concerning the applied voltage, the electrical cell power (P) required for the reaction at the experimental electrodes is calculated using the equation [31] :

$$P = I * V \quad \ldots (4)$$

$$R = \frac{V}{I} \quad \ldots . (5)$$

Calculating the power ohmic loss (P_{loss}) is another vital parameter to assess cell performance, and it is depicted as the following [30]:

$$P_{loss} = I^2 * R_{loss} \quad \ldots . (6)$$

$$R_{loss} = \frac{V_{final} - V_{initial}}{I_{final} - I_{initial}} \quad \ldots . (7)$$

$$\eta = \frac{P - P_{loss}}{P} * 100 \quad \ldots .. (8)$$

Where

V = the applied voltage (volt)
I = the current flowing through the cell (A)
R = the resistance of the cell (Ω)
P_{loss} = ohmic power loss (W)
V_{final}, $V_{initial}$, I_{final}, $Initial$ = parameters estimated from the I-V curve

The volume of the produced hydrogen is proportional to the passed current and can be calculated as the following [32]:

$$Vol_{H_2} = \frac{I * t * V_m}{n * F} \quad \ldots . (9)$$

Where

I = the cell current in amperes, t is the time in seconds
V_m = molar volume (24710 cm^3/mole)
F = the Faraday constant (96500 Cloumb/mol)
n= is the number of the required electrons

3- Electrolyzer system description

Fig. 3 shows a schematic diagram for the electrolysis system and associated devices. The one-liter plastic basin was used as a container for 10, 20, and 30 % KOH electrolytic solutions (PH=13). Two plastic bottles (50 ml) were used as a gas separator and collector for the produced hydrogen and oxygen, which directed the hydrogen gas to flow into the atmosphere. Two holes were drilled at the bottom of the basin in which rubber plugs were used to hold the electrodes tightly. A distance of 4 cm between both electrodes has been fixed. Flexible tubes were used to transfer the hydrogen gas from the electrolyzer to the vent. Temperature data logger type Applent (model AT4532) Multi-Channel and regular DC Power Supply (model APS3005S) from ATTEN were used for measuring electrolyte temperature and power consumption, respectively. Two main parameters were measured during each experiment: voltage and current. The prototype is designed to test Two metal electrodes, Ti and Ni, under different operating conditions like the voltage, current, and KOH concentrations. Six experiments with three different KOH concertation of 10, 20, and 30 % are carried out in a manner where the Ti metal is fixed as an anode. The cathode is alternately Ti in the former experiment and Ni in the next experiment of the same KOH concentration. The seventh experiment is designed in inverse arrangement, i.e. Ti (cathode)-Ni (anode). The first purpose of those different configurations is to investigate their capacity for supplying hydrogen gas directly related to the optimal metal electrode. The second purpose is to monitor the behavior of each electrode, Ti or Ni, toward the water electrolysis, gas bubble velocity, and electrolyte temperature when different cell voltages are applied.

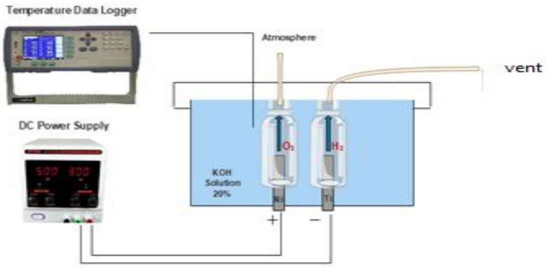

Fig. 3: Schematic diagram of the experimental setup for electrolysis cell

4- Results and discussion

The surface morphology of Ni and Ti electrodes is shown in Fig.4 (left column). The SEM images took out at a magnification of 1000X for each sample. The Ni substrate shows nanoparticles uniformly cover the surface and form approximately irregular spheres or platelets with few agglomerates. The SEM image shows that the platelet's shapes are formed probably due to agglomeration. with different concentrations and non-uniform dispersion. The pure Ti surface with a smooth film consisting of agglomerated fine nanoparticles due to the formation of a native film of TiO_2 can be observed clearly. These fine particles on the Ti substrate disappeared when Ti oxides with Ti indicating that TiO_2 nanoparticles covered the substrate. The chemical constituents in the metals Ni and Ti are also shown in Fig. 4 (right column). The weight percentage of O elements as estimated from EDS analysis is the highest for the Ni electrode (6.3 %) followed by the pure Ti electrode (5.4 %). According to the interpretations above, the chemical precipitation of O on the Ni and Ti substrates is the most active surface area for water molecule adsorption and decomposition on the surface. EDS technique also showed that 76.8 % of Ni and 67 % of Ti elements are presented on Ni and Ti substrates, respectively, providing sufficient sites for electrons to move for the reduction of hydrogen protons. The analysis of surface composition shows the existence and distribution of impurities for the two selected electrodes. The impurities (K, Cl, Mo, and Na) shown in the EDS results can be attributed to the presence of impurities in the precursor materials used during the preparation of electrodes. The Au percent shown in all samples is most likely applied during the sample preparation process for SEM imaging. Also, the carbon percent found in the elemental analysis of all substrates is probably due to the carbon tab used as a support for the substrates. Thus, EDS analysis confirmed that Ni, Ti, and O are present on the electrodes.

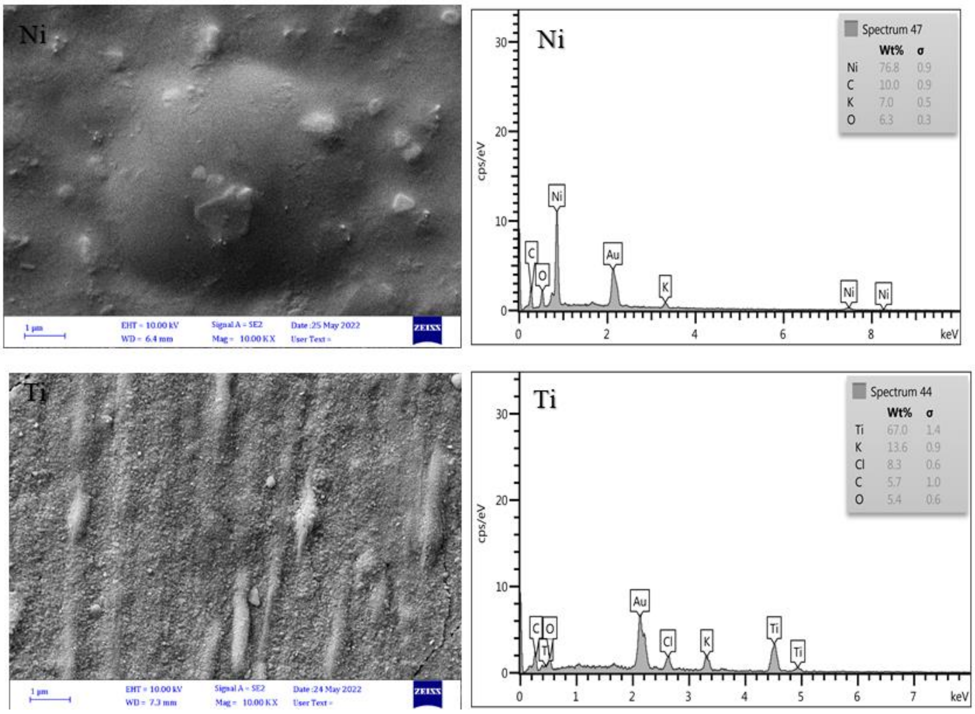

Fig. 4: SEM images and EDS analysis for Ni and Ti metals

As the driving force, the cell voltage is very important to the water electrolysis system. A high cell voltage causes a large current lift for the system at the same system temperature. Then, the large current lift results in a high hydrogen production capacity. Fig. 5 illustrates the polarization curves of the selected electrodes with different inlet cell voltages and different KOH solution weight percentages of 10, 20, and 30 % (wt/wt). According to this figure, two linear zones can be distinguished; the first zone is before 3 V (activation zone) and the second zone is after 3 V (ohmic loss zone). All samples have similar polarization trends and the cell voltage rises linearly before the first 3 V, but after 3 V, this rising curve slope increases gradually. For all experiments, the Ti-Ti system showed a higher voltage in the solution of 10 % KOH, a close voltage in 20 % KOH, and a lower voltage in 30 % KOH compared with the system of Ni-Ti. This phenomenon can be attributed to the activity of the oxidation state of Ti metal (+2, +3, and +4) being higher than that of Ni (+2 and +3), and this activity increases with the KOH concentration. On the other perspective, both Ni-Ti and Ti-Ti systems of 30 % KOH show the lowest voltage followed by the system of 20 % KOH and then by the system of 10 % KOH. Therefore, working on a higher KOH concentration tends to decrease the cell voltage to the minimum and, consequently, it results in increasing the current during the water splitting process which in turn increases the hydrogen reaction rate. Thus, the electrolyte concentration has a significant effect on which the best choice of cathode and anode materials. For example, Ni-Ti electrodes showed a better response when the electrolyte concentration is 10 % while Ti-Ti electrodes showed better performance at 30 % KOH, and a similar I-V behavior for both metals can be noted when the 20 % KOH solution is used. Using these results, it was determined that the electrolyte concentration strongly affected the fixing of the Ti or Ni as one is the cathode and the other is the anode. The I-V curves of water electrolysis on Ti-Ni, Ti-Ti, and Ni-Ti are presented in Fig. 6. The experimental results include the use of 20 % KOH solution when all samples were exposed to a maximum high current of 5 A at an operating temperature of 20.3°C. It is shown that both systems of the Ti-Ti or Ni-Ti show a low voltage compared with the system of Ti-Ni. Therefore, it is preferred to install the Ni metal as a cathode and Ti metal as an anode, because this decrease in low voltage will influence the performance of the electrolyzer capacity. Moreover, it can be seen the activation zone for the Ti-Ni system is shorter than for the Ni-Ti system. This phenomenon indicated that the transfer of electrons from the electrolyte to the electrode and vice versa is faster when the Ni substrate is employed as an anode rather than as a cathode.

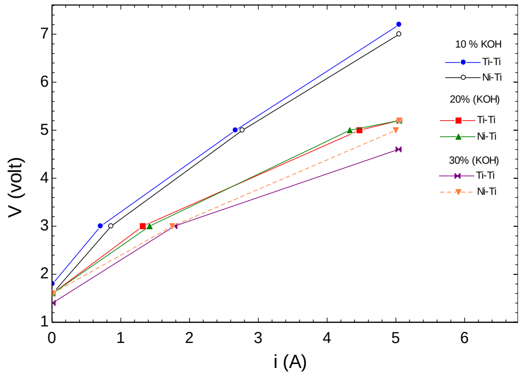

Fig. 5: I-V curves of the Ti and Ni electrodes at different electrolyte concentrations

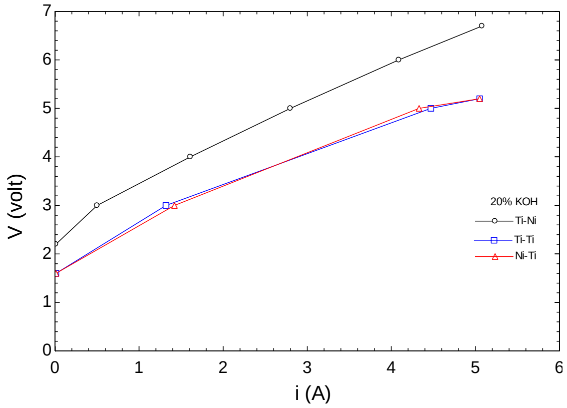

Fig. 6: comparison of the Ti and Ni electrodes at different locations

Fig. 7 shows the electrolyzer resistance change in different amounts of electrolyte concentrations measured at various passed currents. These resistance values give a clear concept of the behavior of each electrode. As seen in this figure, the value of system resistance for all samples decreases with the passed current for the same electrolyte concentration but decreases linearly when the electrolyte concentration is 20 and 30 % KOH. This difference in resistance curves indicates that the electrode is working with a good ions movement and an adequate conductivity of the KOH electrolyte is generated due to the increase in the cell voltage of the system.

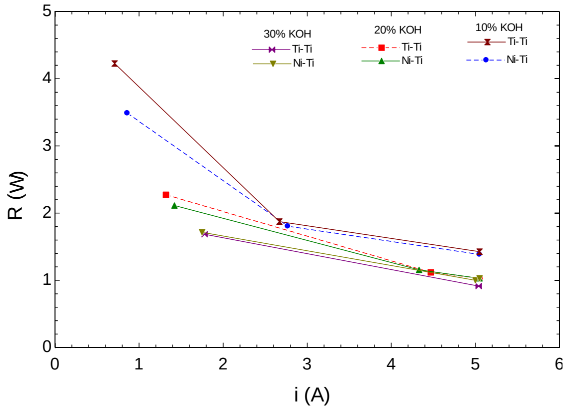

Fig.7: cell resistance curves

Two types of reactions occur in water electrolysis: endothermic and exothermic. An endothermic reaction absorbs or uses heat from its surroundings. Inversely, an exothermic reaction releases heat to its surroundings. During electrolysis, heat is given to the water, which gets absorbed by water to give oxygen and hydrogen, so the reaction is endothermic. Without a doubt, the electrolyte temperature is thermodynamically a dependable parameter for describing the transfer of heat from/to the water electrolysis system. It should not be neglected in testing an electrolyzer, especially when the temperature is decreasing because the current decreases and could not be sufficient or stable due to the variation of the electrolyte conductivity which is strongly affected by its temperature. According to Fig. 8, the electrolyte temperature of the Ti-Ti system is moving toward stability after the elapse of 60 mins, then there is a very little decrease within a specified period, and it will return to stability again for longer than 120 mins while the electrolyte temperature of the Ni-Ti system still decreases gradually with the progress of time. The possible reason is that at the start of the electrolysis process, the electrolyte has a certain temperature, so heat can easily be adsorbed from the electrolyte with little amount. As the process of water splitting goes on, electrolyte temperature declines, and so does the rate of current. In the Ni-Ti system, the amount of heat transfer is the highest, so the highest current rate is required to compensate for the heat loss. Using these results, it can be concluded that the system of Ni-Ti will be the optimum for the water-splitting reaction, leading to more hydrogen production. Similar behavior of electrolyte temperature was noted in systems of 20 and 30 % KOH solutions. From a chemical viewpoint, an endothermic reaction is accompanied by a decrease in the temperature of the electrolyte mixture. Thus, in the electrolysis process, more energy is absorbed when the bonds in the water are broken than is released when new bonds of hydrogen gas are formed.

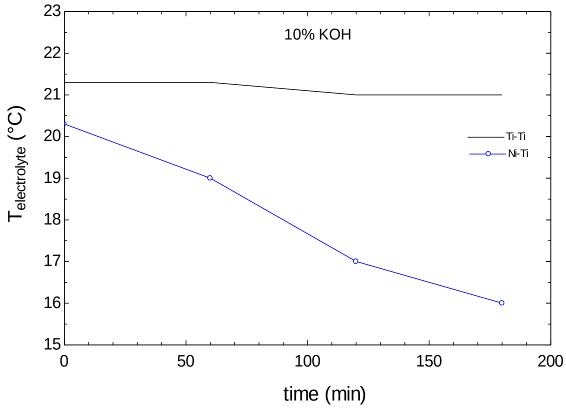

Fig. 8: variation of the electrolyte temperature with time

In Fig. 9, we have reported the experimental results that have been done to discover the deviation of the passed current with the operating time when a constant voltage of 3 V is applied. The comparison among these figures shows a sharp decline in current for Ti-Ti and Ni-Ti substrates with time for all concentrations of KOH solutions. The rated current decreased when the temperature was lowered (Fig. 8), which means that the water electrolysis was taking a long time at lower currents. The contact resistance between the electrolyte and the electrode, the electrolyte concentration, the distance between the electrodes, and the low conductivity of the electrolyte cause this decline in the current between the initial current and the rest current throughout the experiment. Moreover, it can be observed that this deviation in current increases with the increase in KOH concentration confirming the loss of more electrons in the higher electrolyte concentration.

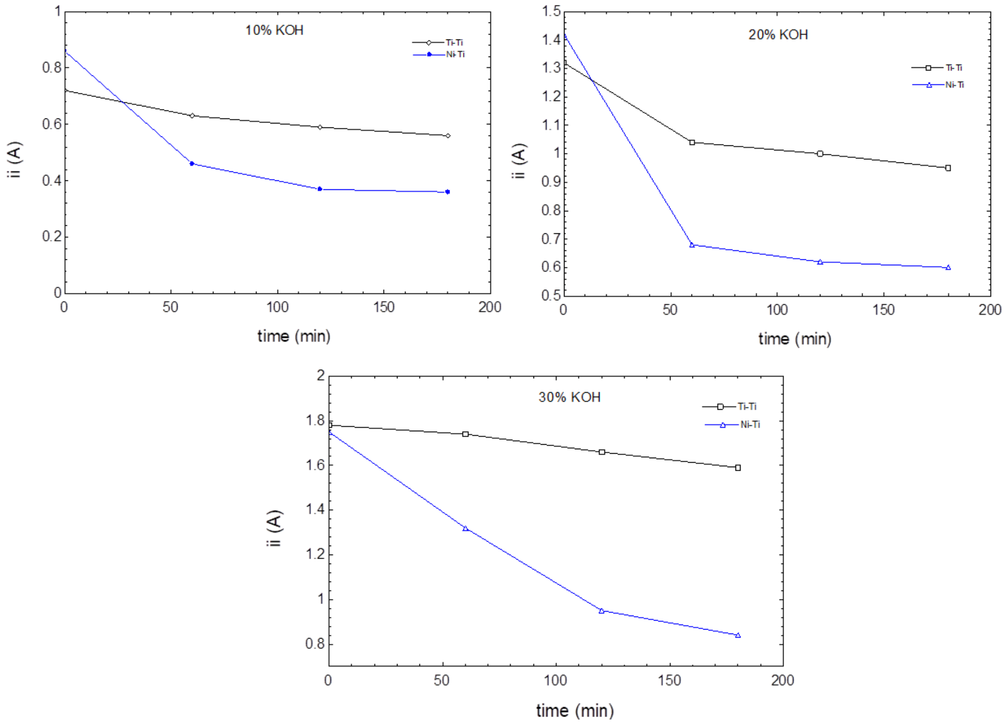

Fig. 9: variation of the cell current with time at a constant voltage of 3 V

Generally, the higher the cell voltage is, the bigger the generation current becomes in unit time. However, the faster migration of electrons and ions is, the higher the hydrogen reaction rate becomes. It is concluded that continuing hydrogen evolution needs a high voltage, especially after the electrolyte temperature, consequently the current, drops to the least value. The calculated values of the hydrogen production as a function of the cell voltage using Ti-Ti and Ni-Ti systems are reported in Fig. 10. The hydrogen production has an optimum value of about 6331 cm^3 at the Ti-Ti (20%KOH) and Ni-Ti (20% and 30 % KOH) when the cell voltage of 5 V is applied; it is noticeably higher than the hydrogen production from the other electrodes at the same voltage of 5 V.

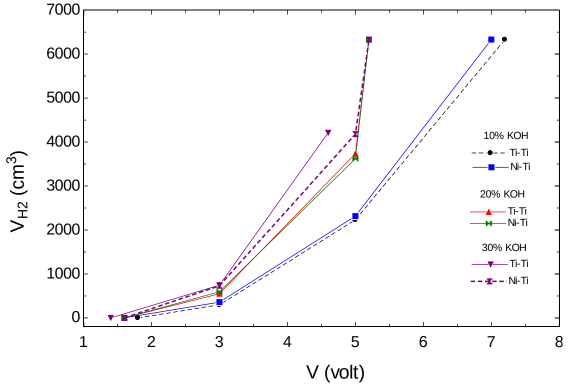

Fig.10 variation of the hydrogen production with the cell voltage

It can also be observed from Fig.10 that during the electrolysis of Ti-Ti (30 % KOH), the hydrogen production doesn't optimally reach the approach rate of hydrogen as shown by its isotope electrode, Ni-Ti (30 % KOH). This may indicate that Ni metal has a large active site surface area for water splitting despite the Ti having a higher oxidation state. Indeed, hydrogen production is affected by other parameters such as the activation potential of the substrates, bubble sizes, and ohmic resistance. Therefore, using the Ti-Ti and Ni-Ti (10 % and 30 % KOH) will be less useful and economic for the electrolysis process, and that will decrease the hydrogen production rate to lower values.

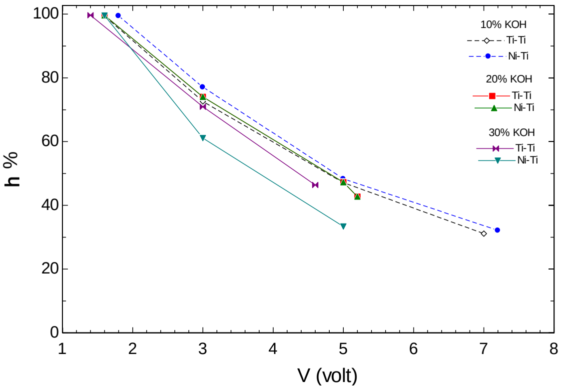

Fig.11variation of the cell efficiency with the voltage

The results of efficiency for six samples of different KOH concentrations are presented in Fig. 11. Under cell voltage of 3 V, the highest efficiency of 72 % was obtained in the case of Ni-Ti (10 % KOH), and the lowest efficiency of 61 % was obtained in the case of Ni-Ti (30 % KOH). The cell efficiency for the symmetrical systems decreased with increasing the KOH concentration. This decrease in efficiency is broadly linked to the power ohmic loss and subsequently hydrogen production. For example, the hydrogen rate and the power ohmic loss were 359 cm^3 and 0.7 w for the Ni-Ti system of 10 % KOH but for the same system of 30 % KOH the results were 731.3 cm^3 and 2 W. These results prove that there is an upper limit for efficiency at a certain hydrogen production rate; thus, beyond this rate, the efficiency would be restrained.

Table 1 summarizes the results of the efficiencies, hydrogen production, and power ohmic loss for the six systems at different concentrations of KOH. It can be observed that the highest power ohmic loss was 17 W (η =35.26 %) for the Ni-Ti system of 30 % KOH, and the lowest power ohmic loss was 6.899 W (η =48.32 %) for the Ni-Ti system of 10 % KOH. The obtained results indicate that more improvement should be done on the Ti and Ni electrodes to increase their performance. Coating with nanomaterials is one of the most common methods that can be used to increase the active surface area on the electrode surface, which, in turn, leads to improving the reaction rate of the hydrogen. It can also be seen that working at a cell voltage of 5 V increased the power ohmic loss, consequently, this increase in power ohmic loss resulted in a decrease in efficiency. In contrast to the results of the power ohmic loss, a higher value of the hydrogen flow rate resulted in higher values of efficiency. The reason behind this is that increasing the cell voltage made the electrolyzer receive a large amount of current during the electrolysis process. This is because the higher the cell voltage is, the bigger the consumption of current becomes. It can be noted that both power ohmic loss and efficiency did reach their maximum values at the same time. But this value is perhaps not the target to get the best efficiency of the electrolyzer, because there are other parameters affecting the efficiency such as electrolyzer production capacity, working time, gas bubbles sizes, produced gas velocity, and stability of the electrolyte temperature.

Table 1: Results of hydrogen production, power ohmic loss, and efficiency at a cell voltage of 5 V

system	% KOH	Cell voltage	Hydrogen production cm^3	Power Ohmic loss w	Efficiency %
Ti-Ti	10	5	2232	6.899	48.32
Ni-Ti	10	5	2315	7.325	47.11
Ti-Ti	20	5	3736	11.78	47.27
Ni-Ti	20	5	3619	11.36	47.52
Ti-Ti	30	4.6	4212	12.43	46.39
Ni-Ti	30	5	4179	17	35.26

compares the findings of this study with those of previous research on AEC systems. It was observed that the use of the stainless-steel electrode resulted in the production of 10 cm^3 of H_2 gas [33]. However, the system's low H_2 output can be attributed to its low applied voltage of 3.4V. Another factor is that the reaction rate was slowed because NaOH has a lower conductivity than KOH. This resulted in a lower electrolytic temperature. Similarly, Mandal et al. used a graphite electrode, but with a membrane at the applied voltage of 5V producing a low H_2 rate of 5 cm^3. The reasons might be the hydrophilicity of the membrane used or the H_2O permeability through that membrane [34].

5- Conclusion

This article showed the possibility of generating hydrogen gas as a source of renewable energy from the Ti-Ni water electrolysis system by employing an alkaline solution medium. Two main metal electrodes, Ti and Ni, with their surface morphology, cell voltage, and KOH mixing ratio were assessed for hydrogen evolution. Concerning hydrogen production of 30% KOH system, Ti-Ti showed the highest hydrogen production of 4212 cm^3 at a cell voltage of 4.6V, while Ni-Ti system produced 4179 cm^3 at 5V. A maximum efficiency accompanied by a minimum power ohmic loss was gotten when the electrolyzer was equipped with Ni-Ti of 20 % KOH solution system. The results proved that the heat transfer is not constant due to the continue decreasing in electrolyte temperature and this phenomenon showed that the reaction of water splitting for the Ni-Ti system is endothermic. The present study shows that the efficiency is strongly influenced by the electrode arrangements of the Ti and Ni and by the concentration of the employed electrolyte. The results can be used to upgrade the modeling and simulation mode of hydrogen to improve the accuracy of predictions. Therefore, the adoption of a Ni-Ti electrolyzer of 20 % KOH concentration is the optimal choice to produce hydrogen from this type of metal substrate.

References

[1] Gandía, L.M.; Oroz, R.; Ursúa, A.; Sanchis, P.; Diéguez, P.M. Renewable Hydrogen Production: Performance of an Alkaline Water Electrolyzer Working under Emulated Wind Conditions. Energy Fuels 2007, 21, 1699–1706.

[2] Suleman, F.; Dincer, I.; Agelin-Chaab, M. Environmental Impact Assessment and Comparison of Some Hydrogen Production Options. Int. J. Hydrog. Energy 2015, 40, 6976–6987.

[3] Santos, D.M.F.; Sequeira, C.A.C.; Figueiredo, J.L. Hydrogen Production by Alkaline Water Electrolysis. Quim. Nova 2013, 36, 1176–1193.

[4] Wang, M.;Wang, Z.; Gong, X.; Guo, Z. The Intensification Technologies to Water Electrolysis for Hydrogen Production—A Review. Renew. Sustain. Energy Rev. 2014, 29, 573–588.

[5] Gahleitner, G. Hydrogen from Renewable Electricity: An International Review of Power-to-Gas

Pilot Plants for Stationary Applications. Int. J. Hydrog. Energy 2013, 38, 2039–2061.

[6] Zeng, K.; Zhang, D. Recent Progress in Alkaline Water Electrolysis for Hydrogen Production and Applications. Prog. Energy Combust. Sci. 2010, 36, 307–326.

[7] Rashid, M.; Mesfer, M.K.A.; Naseem, H.; Danish, M. Hydrogen Production by Water Electrolysis: A Review of Alkaline Water Electrolysis, PEM Water Electrolysis and High Temperature Water Electrolysis. Int. J. Eng. Adv. Technol. 2015, 4, 80–93.

[8] Götz, M.; Lefebvre, J.; Mörs, F.; McDaniel Koch, A.; Graf, F.; Bajohr, S.; Reimert, R.; Kolb, T. Renewable Power-to-Gas: A Technological and Economic Review. Renew. Energy 2016, 85, 1371–1390.

[9] Ehret, O.; Bonhoff, K. Hydrogen as a Fuel and Energy Storage: Success Factors for the German Energiewende. Int. J. Hydrog. Energy 2015, 40, 5526–5533.

[10] Leonardo Vidas and Rui Castro. Recent Developments on Hydrogen Production Technologies: State-of-the-Art Review with a Focus on Green-Electrolysis. Appl. Sci. 2021, 11, 11363. https://doi.org/10.3390/app112311363.

[11] Nikolaidis, P.; Poullikkas, A. A comparative overview of hydrogen production processes. Renew. Sustain. Energy Rev. 2017, 67, 597–611.

[12] Escobedo, S.; Serrano, B.; Calzada, A.; Moreira, J.; de Lasa, H. Hydrogen production using a platinum modified TiO2 photocatalyst and an organic scavenger. Kinetic modeling. Fuel 2016, 181, 438–449.

[13] Sapountzi, F.M.; Gracia, J.M.; Weststrate, C.K.J.; Fredriksson, H.O.; Niemantsverdriet, J.H. Electrocatalysts for the generation of hydrogen, oxygen and synthesis gas. Prog. Energy Combust. Sci. 2017, 58, 1–35.

[14] Choi, H.; Kim, J.; Kim, H.; Lee, S.; Lee,Y. Improving the Electrochemical Performance of Hybrid Supercapacitor usingWell-organized Urchin-like TiO2 and Activated Carbon. Electrochim. Acta 2016, 208, 202–210.

[15] Liu B, He J-B, Chen Y-J, Wang Y, Deng N. Phytic acid-coated titanium as electrocatalyst of hydrogen evolution reaction in alkaline electrolyte. Int J Hydrog Energy 2013;38:3130-6.

[16] Xiang Song, Hui Zhao, Keneng Fang, Yongshan Lou, Zongkui Liu, Chifeng Liu,Zhandong Ren, Xiaorong Zhou, Hua Fang and Yuchan Zhu. Eff ect of platinum electrode materials andelectrolysis processes on the preparation of acidicelectrolyzed oxidizing water and slightly acidicelectrolyzed water. RSC Adv.,2019,9,3113–3119.

[17] Birg¨ul YAZICI. Hydrogen Evolution at Platinum (Pt) and at Platinized Platinum (Ptz) Cathodes. Turk J Chem 23 (1999), 301 – 308.

[18] Maximilian Bernt, Armin Siebel, and Hubert A. Gasteiger. Analysis of Voltage Losses in PEM Water Electrolyzers with Low Platinum Group Metal Loadings. Journal of The Electrochemical Society 2018, 165 F305.

[19] Brauns, J., & Turek, T. (2020). Alkaline Water Electrolysis Powered by Renewable Energy: A Review. Processes, 8(2), 248. doi:10.3390/pr8020248.

[20] Koj, M.; Qian, J.; Turek, T. Novel Alkaline Water Electrolysis with Nickel-Iron Gas Diffusion Electrode for Oxygen Evolution. Int. J. Hydrog. Energy 2019, 44, 29862–29875.

[21] Amin, M. A., Fadlallah, S. A., & Alosaimi, G. S. (2014). In situ aqueous synthesis of silver nanoparticles supported on titanium as active electrocatalyst for the hydrogen evolution reaction. International Journal of Hydrogen Energy, 39(34), 19519-19540. doi:10.1016/j.ijhydene.2014.09.100.

[22] Rauscher, T.; Bernäcker, C.I.; Mühle, U.; Kieback, B.; Röntzsch, L. The Effect of Fe as Constituent in Ni-Base Alloys on the Oxygen Evolution Reaction in Alkaline Solutions at High Current Densities. Int. J. Hydrog. Energy 2019, 44, 6392–6402.

[23] Amin MA, Fadlallah SA, Alosaimi GS. Activation of titanium for synthesis of supported and unsupported metallic nanoparticles. J Electrochem Soc 2014;161:D672-80.

[24] Sekimoto H, Uda T, Nose Y, Sato S, Awakura Y. Reduction of titanium oxide in the presence of nickel by nonequilibrium hydrogen gas. J Mater Res 2009;24:2391-9.

[25] Padmos JD, Duchesne P, Dunbar M, Zhang P. Gold nanoparticles on titanium and interaction with prototype protein. J Biomed Mater Res A 2010;95:146-55.

[26] Alejandro N. Colli, Hubert H. Girault and Alberto Battistel. Non-Precious Electrodes for Practical Alkaline Water Electrolysis. Materials 2019, 12, 1336; doi:10.3390/ma12081336.

[27] Cinthia Alegre, Stefania Siracusano, Esterina Modica, Antonino S. Aricò, Vincenzo Baglio. Titanium–tantalum oxide as a support for Pd nanoparticles for the oxygen reduction reaction in alkaline electrolytes. Materials for Renewable and Sustainable Energy (2018) 7:8 https://doi.org/10.1007/s40243-018-0114-z.

[28] Wang H, Zhang XF, Zhai SS, Yuan JJ, Wang WC, Zhu YW, et al. Research Note: The comparative study of energy utilization in feedstuffs for Muscovy ducks between in vivo and in vitro. Poult Sci. 2021;100(2):1004-7.

[29] Hossain FM, Sheppard L, Nowotny J, Murch GE. Optical properties of anatase and rutile titanium dioxide: Ab initio calculations for pure and anion-doped material. Journal of Physics and Chemistry of Solids. 2008;69(7):1820-8.

[30] Esposito E, Minotti A, Fontananova E, Longo M, Jansen JC, Figoli A. Green H2 Production by Water Electrolysis Using Cation Exchange Membrane: Insights on Activation and Ohmic

Polarization Phenomena. Membranes (Basel). 2021;12(1).

[31] Rodziewicz, J., Mielcarek, A., Janczukowicz, W., & Bryszewski, K. Electric Power Consumption and Current Efficiency of Electrochemical and Electrobiological Rotating Disk Contactors Removing Nutrients from Wastewater Generated in Soil-Less Plant Cultivation Systems. Water, 2020, 12(1), 213 http://doi:10.3390/w12010213.

[32] M. Kaddami and M. Mikou, Science Direct Effectof operating parameters on hydrogen productionby electrolysis of water, Int. J. Hydrogen Energy, 2017, 42, 40:. 25550–25557.

[33] de Fátima Palhares, D. D. A., Vieira, L. G. M., & Damasceno, J. J. R. (2018). Hydrogen production by a low-cost electrolyzer developed through the combination of alkaline water electrolysis and solar energy use. International Journal of Hydrogen Energy, 43(9), 4265-4275.

[34] Mandal, B., Sirkar, A., De, P., & Kuila, S. B. (2016). Studies on the Effect of Electrolyte Concentration on Alkaline Electrolysis and Ion Exchange Membrane Water Splitting For Production of Hydrogen. International Journal of Research in Engineering and Technology

دراسة مقارنة لمعدن النيكل ومعدن التيتانيوم لتفاعل تطور الهيدروجين في التحليل الكهربائي للماء

آية أواس سعد ، فرقد علي لطيف

قسم هندسة الطاقة ، كلية الطاقة ، جامعة بغداد ، بغداد ، العراق

الملخص

يبحث هذا العمل تجريبيًا ونظريًا في تغير خرج I-V ، وإنتاج الهيدروجين ، وكفاءة معادن Ti و Ni كركائز لأنظمة التحليل الكهربائي للماء. لإجراء التحسين بين الأقطاب الكهربائية المرشحة ، تم استعمال سبعة تكوينات من Ni-Ti و Ti-Ti و Ti-Ni ضمن ثلاثة محاليل الكتروليتية لهيدروكسيد البوتاسيوم بنسب وزنية مكونة من 10 و 20 و 30٪ . كنظام كاثود–أنود. تم فحص الأقطاب الكهربائية المختارة عن طريق المسح المجهري الإلكتروني (SEM) والأشعة السينية المشتتة للطاقة (EDX) لدراسة التشكل السطحي وتكوين العناصر لهذه المعادن. أظهرت النتائج التجريبية أن Ni-Ti وTi-Ti ضمن نسبة 20 و 30٪ لمحلول هيدروكسيد البوتاسيوم كان الأعلى في معدل انتاج الهيدروجين. في المقابل ، أظهر نظام Ti-Tiلمحلول 10 ٪ هيدروكسيد البوتاسيوم أعلى كفاءة مع أقل خسارة أومية ، مما يشير إلى أن المحلل الكهربائي يمكن أن يتأثر بشدة بتركيز محلول هيدروكسيد البوتاسيو . حيث ان زيادة تركيز الإلكتروليت جعلت التيار المار أقل استقرارًا وينخفض بمرور الوقت ، مما يجعله مناسبًا للعمل بجهد خلية أقل وفقدان طاقة أومية اقل أيضا, ولكن مع إنتاج منخفض للهيدروجين. يُظهر انخفاض درجة حرارة جهاز التحليل الكهربائي مع تفاعل تجزئة الماء أن هذا النوع من التفاعل ماص للحرارة. توضح هذه الدراسة أيضا أن نظام Ni-Ti يمكن أن يكون المصدر الأكثر ملاءمة لتطور الهيدروجين بدلاً من الترتيبات الأخرى عندما يتم تحضير نسبة الخلط المناسبة التي تبلغ 20٪ من محلول هيدروكسيد البوتاسيوم قبل عملية التحليل الكهربائي.